Biochimica et Biophysica Acta, 1105 (1992) 278–284

BBAMEM 75582

The influence of Mg^{2+} on anion binding to sarcoplasmic reticulum membranes as detected by ^{35}Cl-NMR

Stefan F. Janetzky, Helmut Hanssum, Gerhard Spatz-Kümbel and Hans G. Bäumert

Institut für Biophysikalische Chemie und Biochemie der Johann-Wolfgang-Goethe-Universität, Frankfurt am Main (Germany)

(Received 11 July 1991)
(Revised manuscript received 14 January 1992)

Key words: Anion binding; Magnesium ion; Phosphate; Pyridoxalphosphate-6-azophenyl-2'-sulfonic acid; Adenylyl imidodiphosphate; Sarcoplasmic reticulum; NMR, ^{35}Cl-

^{35}Cl-NMR spectroscopy has been used to study the competition between anions, including nucleotides, on skeletal muscle sarcoplasmic reticulum membranes. Different chloride binding sites can be distinguished according to their Mg^{2+} sensitivity. Phosphate binding is enhanced by Mg^{2+} whereas the anion transport inhibitor pyridoxalphosphate-6-azophenyl-2'-sulfonic acid (PPAPS) binding is not. The affinity of the enzyme for the Mg-adenylyl imidodiphosphate (MgAMP-PNP) complex is decreased whereas that for MgATP is increased. Three sets of binding sites can be discriminated from which chloride is displaced by different anions with varying efficiency. High affinity binding of AMP-PNP and PPAPS occurs at the same site, that can also be occupied by phosphate. Low-affinity binding of PPAPS and AMP-PNP also coincides, but in a site where phosphate binding is negligible. ATP and ADP bind to both sites. In the presence of Mg^{2+} a third anion binding site can be occupied by phosphate but neither by AMP-PNP nor PPAPS.

Introduction

Mg^{2+} plays a central role concerning several functions connected with the transfer of Ca^{2+} across the sarcoplasmic reticulum membrane. Thus, the true substrate for the Ca^{2+}-ATPase and the driving force for the Ca^{2+}-pumping process is the magnesium complex of ATP [1–3]. During the catalytic cycle Mg^{2+} accelerates both phosphorylation and dephosphorylation of the Ca^{2+}-pump [4–6]. At the end of one transport cycle Mg^{2+} and ATP promote the conversion of the enzyme from the E_2 to E_1 conformation [7], and a new catalytic and transport cycle begins. Mg^{2+} also enhances the binding of phosphate to the Ca^{2+}-ATPase (and vice versa), although the free phosphate and not the Mg^{2+}-phosphate complex is the true substrate for phosphoprotein formation both, in the presence and absence of a transmembrane Ca^{2+} gradient [8–10]. The Ca^{2+}-dependent Ca^{2+}-release [11,12] mediated by the ryanodine receptor of junctional terminal cisternae is inhibited by 3 mM Mg^{2+}.

Rousseau [13] and Rousseau et al. [14] using the bilayer technique found that there is no influence of Mg^{2+} or ATP on the chloride channels of sarcoplasmic reticulum membranes, whereas Beil et al. [15], and others [16–18] reported that the anion transport associated with the transport of Ca^{2+} across the SR membrane is Mg^{2+}-dependent.

We were interested whether it is possible to detect any influence of Mg^{2+} on anion binding to the sarcoplasmic reticulum membrane by ^{35}Cl-NMR, as this may provide new information about the relationships between anion binding and the Mg^{2+}-dependent functions of SR mentioned above. ^{35}Cl-NMR has been used in analyzing anion binding to the band 3 protein of the erythrocyte membrane [19], to dromedary haemoglobin [20], and to Photosystem II membrane fragments [21]. In two previous publications [22,23] we have already shown that anion binding to the SR can be monitored by this method.

Abbreviations: AMP-PNP, adenylyl imidodiphosphate; EGTA, ethylenediamine-*N*,*N*'-tetraacetic acid; PPAPS, pyridoxalphosphate-6-azophenyl-2'-sulfonic acid; SDS-PAGE, sodium dodecylsulfate polyacrylamide gelelectrophoresis; SR, sarcoplasmic reticulum; TEA, triethanolamine.
Enzyme: Ca^{2+}-ATPase (EC 3.6.1.38)

Correspondence: H.G. Bäumert, Institut für Biochemie der J.-W.-Goethe-Universität, Haus 75 A, Universitätsklinikum, Theodor-Stern-Kai 7, D-6000 Frankfurt am Main 70, Germany.

Experimental procedures

Materials

AMP-PNP and phospholipids were purchased from Sigma Chemie GmbH (Deisenhofen). ATP (potassium-salt) was from Boehringer Mannheim GmbH (Mannheim), $^{45}CaCl_2$ was from NEN (Dreieich), $^{2}H_2O$, EGTA, triethanolamine and inorganic salts were obtained from E. Merck (Darmstadt). PPAPS was synthesized according to Ref. 22. Asolectin from soybean was purchased from Fluka BioChemika (Neu-Ulm). All chemicals were of purest grade available from the respective companies.

Sarcoplasmic reticulum vesicle preparation

Sarcoplasmic reticulum vesicles were prepared from rabbit hind leg muscle according to Hasselbach and Makinose [24] as modified by De Meis and Hasselbach [25]. The pellet after the last centrifugation (80000 × *g*) was resuspended in 100 mM KCl buffered with 1 mM triethanolamine-HCl (pH 7.4). After homogenization aliquots of the SR suspension (between 10 and 20 mg protein/ml) were shock-frozen in liquid nitrogen an kept in deep freeze at − 70°C. The protein composition of each SR preparation was checked by SDS-PAGE [26], the total protein concentration was determined by a modified Biuret method [27]. The ATPase activity was measured by the method of Fiske and SubbaRow [28] in a phosphate auto-analyzer (Technicon) resulting in an average activity of 1 μmol P_i liberated per minute and mg protein (20°C). The ATP-driven calcium uptake was measured with $^{45}Ca^{2+}$ as radioactive tracer using the filter assay method of Martonosi and Feretos [29]. Maximum Ca^{2+} uptake amounted to 1 μmol Ca^{2+} mg^{-1} min^{-1} (20°C).

^{35}Cl- and ^{31}P-NMR measurements

NMR measurements were carried out on a Bruker AM 270 NMR spectrometer. Details have been described previously [23]. We have conclusively shown that all measurements were under the conditions of fast exchange and that only anion binding sites on the outside of SR vesicles contribute to the observable line broadening. Thus, the titration of sarcoplasmic reticulum vesicle suspensions with chloride results in a superposition of hyperbolic functions provided that the binding constants of different binding sites remain unchanged during titrations. This condition is obeyed above 17 mM KCl where we observe decreasing line width caused by increasing chloride concentrations [23]. We carried out all titrations in the presence of 40 mM chloride assuring sufficient occupation of all anion binding sites by chloride. The sample tube contained for each measurement 5 mg/ml SR vesicle protein. 1 mM TEA-buffer (pH 7.4), 20% (v/v) $^{2}H_2O$ for frequency lock and 10 μM EGTA to keep the free calcium concentration low. Some titrations were performed in the presence of 10 mM of either, free or total magnesium, as described in the legends. The total volume was 2.4 ml. Protein dilution during the titration steps was corrected by appropriate factors and chloride and magnesium concentrations were kept constant. Line broadening ($\Delta\nu$) is defined as the difference of the ^{35}Cl line widths in the presence and absence of SR vesicles, respectively [30].

^{31}P-NMR measurements were carried out at 109.35 MHz using a 10 mm broad band probe to determine the stability of ATP under the conditions used. The number of data points was 8K, the spectral width 55.1 ppm. To determine the intensities of ATP-, ADP-, and P_i-resonances correctly a sufficient delay was introduced between scans. Concentrations were determined by integration.

SR vesicles (5.5 mg protein/ml) containing 10 mM Mg^{2+} and no added Ca^{2+} were incubated with 5 mM ATP. At 5-min intervals ^{31}P-NMR spectra were taken.

Results and Discussion

Influence of Mg^{2+} on anion binding

Vetter et al. in previous communications [22,23] showed that chloride binds to anion binding sites on the SR membrane, from which it can be displaced by phosphate. Since magnesium ions play an essential role in various functions of SR, we were interested if Mg^{2+} would influence the anion binding.

Our first aim was to find out if there was any difference in chloride displacement by phosphate from the phosphate-sensitive binding sites as the function of Mg^{2+} concentration. Fig. 1 shows phosphate titrations of SR vesicle suspensions in the presence and absence of Mg^{2+} analyzed by ^{35}Cl-NMR. Decrease of line width, i.e. decrease of chloride binding in the absence of Mg^{2+} mainly occurs in a concentration range up to 25 mM phosphate. Addition of Mg^{2+} increases the ^{35}Cl line width throughout the whole course of the phosphate titration. The free Mg^{2+} concentration (10 mM) was kept constant. Apparently, the titration in the presence of Mg^{2+} produces a greater amount of chloride displacement. Both curves can be fitted by single hyperbolae according to the following equation:

$$\frac{\Delta\nu}{[P]} = \frac{a \cdot n}{K + [Cl^-] + [I] \times K/K_I} + C$$

It has been derived from Eqn. 2 in Ref. 22. K is the dissociation constant of chloride, K_I the dissociation constant of the inhibitor (inhibitor constant) and C the asymptotic value of the titration curve.

The phosphate K_I values were evaluated as 5.8 ± 2 and 8.8 ± 2 mM (S.D.) in the absence and presence of Mg^{2+}, respectively. These values are comparable to the value of 10 mM found by De Meis [31].

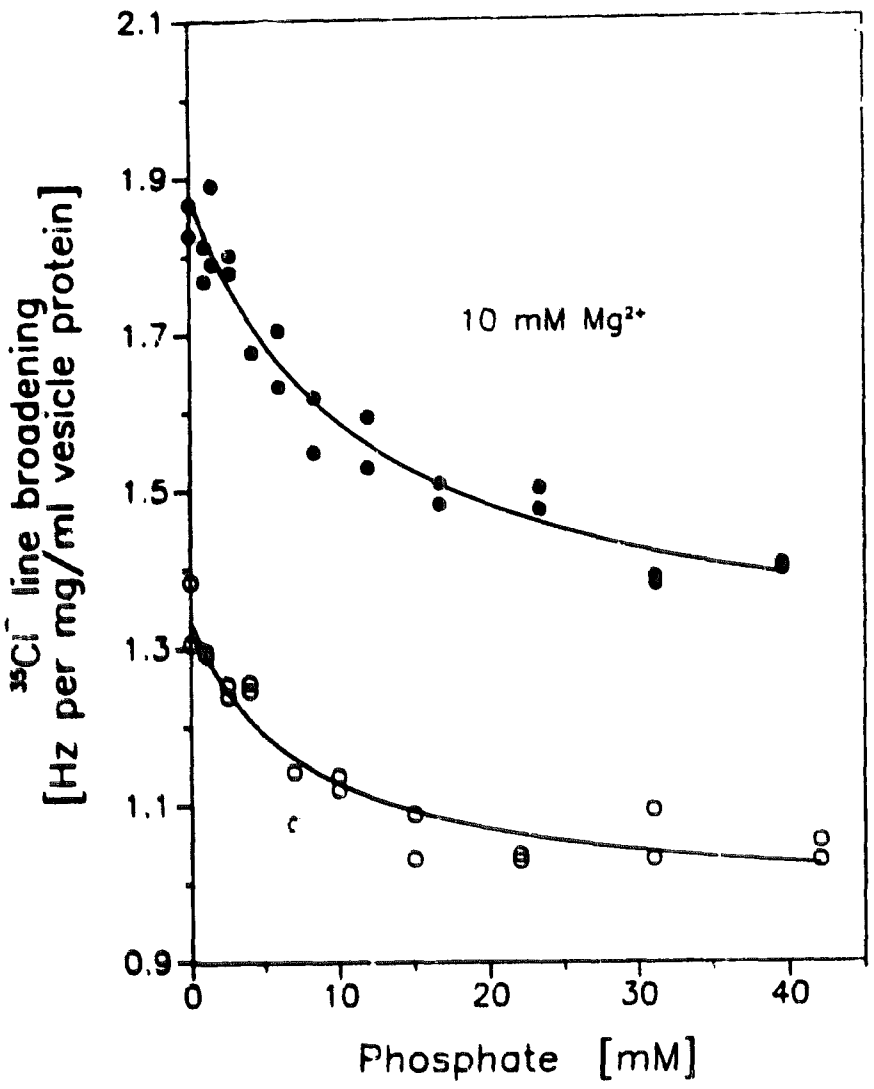

Fig. 1. Dependence of ^{35}Cl line broadening on the free phosphate concentration. ●, Presence of 10 mM free Mg^{2+}; ○, absence of Mg^{2+}. Line broadening was calculated as the difference of ^{35}Cl line width in the presence and absence of SR vesicles devided by the protein concentration. The chloride concentration (40 mM) was kept constant.

The most direct way to investigate the quantitative influence of Mg^{2+} on anion binding to the SR membrane is by titration with Mg^{2+}. The upper curve in Fig. 2 shows increasing line width with increasing Mg^{2+} concentration which indicates that Mg^{2+} enhances chloride binding to the SR membrane. This is half-maximally achieved at 3 mM Mg^{2+}. In a control experiment we titrated Mg^{2+} into solutions of vesicles reconstituted from either, isolated SR lipids or phospholipids, to find out if there was any contribution to the chloride line broadening by the interaction of Mg^{2+} with membrane components other than protein. Indeed, we found a linearly increasing and reproducible enhancement of chloride line width obviously brought about by direct interaction of Mg^{2+} with the protein-free membrane surface (details not shown). This effect proved to be relatively small (e.g. 10% at 15 mM Mg^{2+}) and was subtracted from all Mg^{2+} titrations shown in Fig. 2. An influence of Mg^{2+} on protein- and lipid-free chloride solutions could not be detected at all.

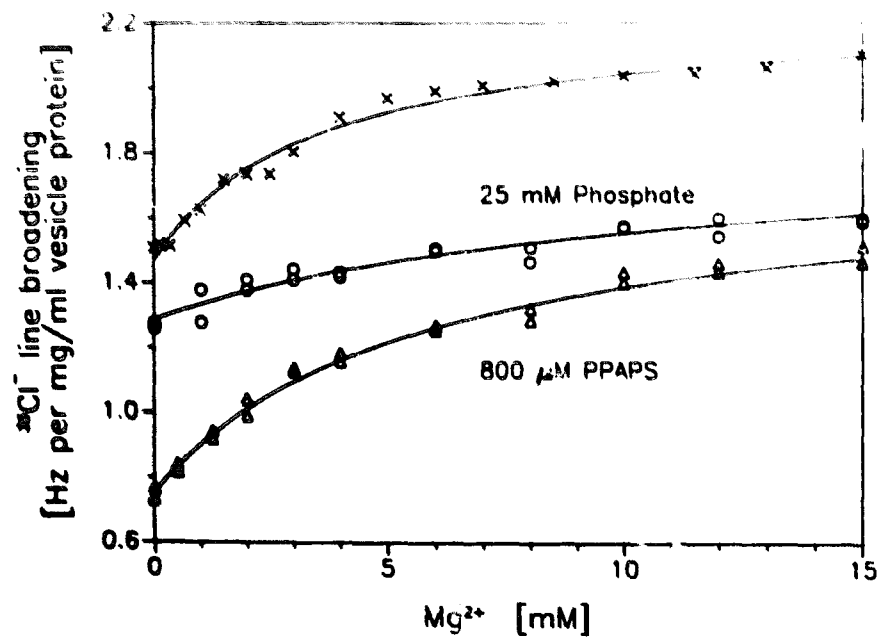

Fig. 2. Influence of Mg^{2+} on ^{35}Cl line broadening. △, Presence of 806 µM PPAPS; ○, presence of 25 mM phosphate; ×, no additions. Corrections concerning the contribution of protein-free vesicles to the ^{35}Cl line width have been made.

The middle curve in Fig. 2 resulted from a Mg^{2+} titration in the presence of 25 mM total phosphate. Under these conditions most phosphate-sensitive anion binding sites should be occupied (see Fig. 1). Therefore, the Mg^{2+} titration shows little increase of line broadening which becomes even smaller when 50 mM phosphate is added. We conclude that most (if not all) of the Mg^{2+}-induced stimulation of anion binding happens at phosphate-sensitive binding sites.

Analysis of PPAPS-sensitive binding sites

The lower curve in Fig. 2 results from a Mg^{2+} titration in the presence of 800 µM pyridoxalphosphate-6-azophenyl-2′-sulfonic acid (PPAPS) which has been used as an inhibitor of anion binding in former ^{35}Cl-NMR studies [22,23]. A large increase of chloride line broadening up to 15 mM Mg^{2+} suggests that PPAPS does not affect Mg^{2+}-sensitive binding sites. These results are also confirmed by the similarity of PPAPS titration curves in the presence and absence of Mg^{2+} as shown in Fig. 3. Both curves show the same chloride displacement caused by PPAPS. The differ-

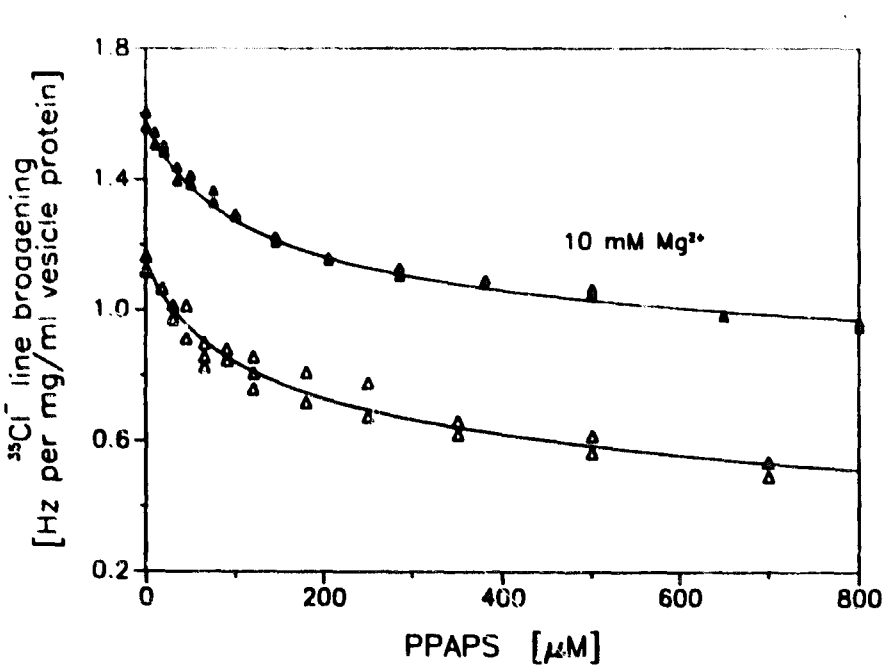

Fig. 3. Titration of PPAPS to a SR vesicle solution. ▲, Presence of 10 mM Mg^{2+}; △, absence of Mg^{2+}.

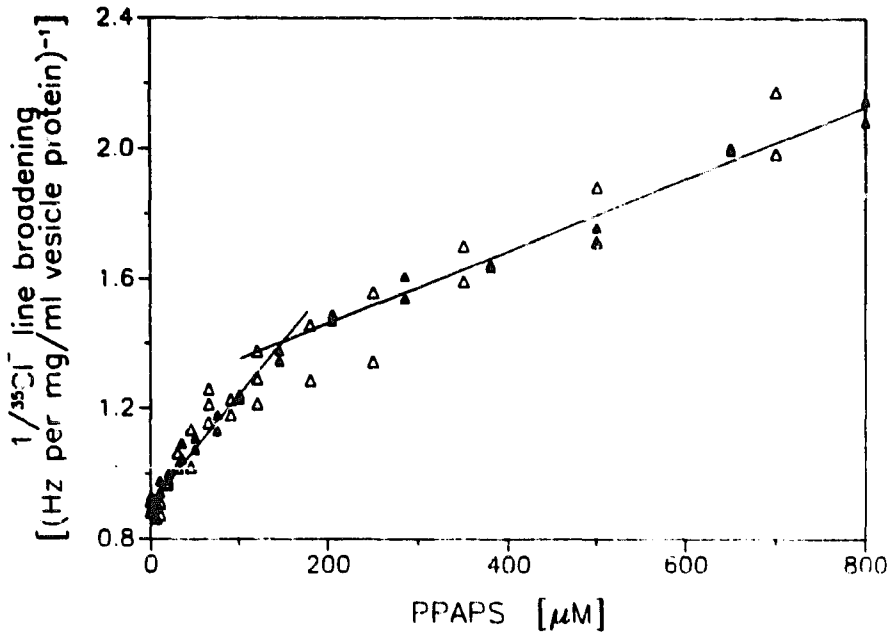

Fig. 4. Semi-reciprocal presentation of the PPAPS titrations. ▲, Presence of 10 mM Mg^{2+}; △, absence of Mg^{2+}. The asymptotic values of the titration curves of Fig. 3 have been subtracted in both cases before inversion.

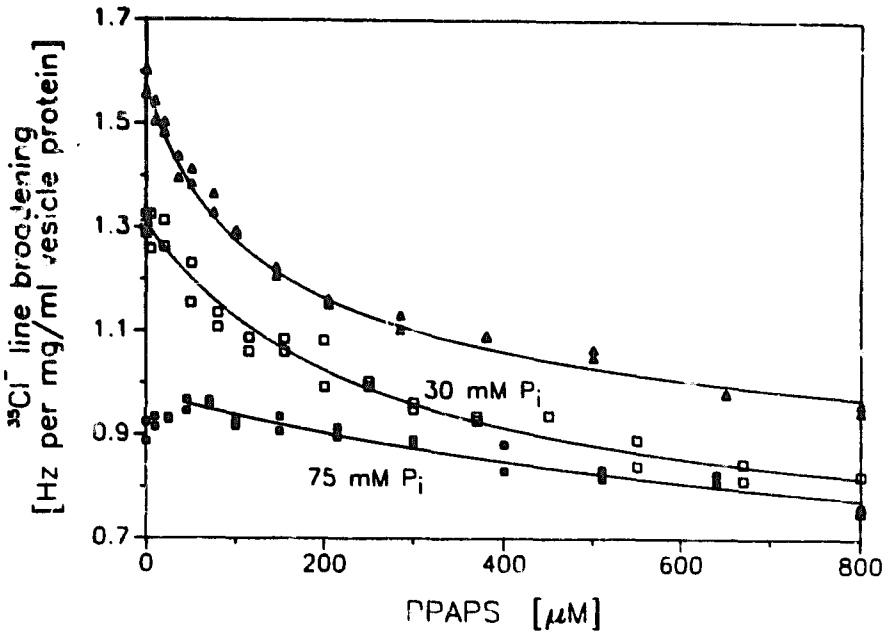

Fig. 5. Titration of PPAPS to SR vesicles as influenced by phosphate. All titrations were performed in the presence of 10 mM total Mg^{2+}. ■, 75 mM phosphate; □, 30 mM phosphate; ▲, without phosphate.

ence in line broadening which is almost the same at any PPAPS concentration is due to the Mg^{2+} effect. The detailed analysis by nonlinear least squares fitting of both data sets showed systematic deviations if only one binding constant was assumed. Using the superposition of two hyperbolae we determined the dissociation constants as well as the theoretical endpoints of the titrations. The K_1 values of PPAPS at the high- and low-affinity binding sites were determined as 45 ± 10 μM and 638 ± 100 μM in the absence of Mg^{2+}, and 58 ± 10 μM and 509 ± 100 μM in the presence of Mg^{2+}, respectively.

Subtracting the asymptotic titration endpoints results in differential curves which describe the displacement of chloride from PPAPS-sensitive binding sites. The semi-reciprocal curves coincide within the limits of experimental error and are biphasic (Fig. 4). This reveals two clearly distinguishable PPAPS binding sites on the SR membrane where chloride binding is not influenced by Mg^{2+}, i.e. Mg^{2+} does not alter the dissociation constants within the limits of experimental error.

Interrelation of phosphate and PPAPS binding sites

To verify the connection of phosphate and PPAPS binding sites [22] we carried out the same titration with PPAPS in the presence of 30 and 75 mM total phosphate and 10 mM total Mg^{2+}. The results are shown in Fig. 5. The addition of 30 mM phosphate reduces chloride binding at all PPAPS concentrations as indicated by the fact that above 300 μM PPAPS the titration curves run parallel. This is also true for a titration in the presence of 75 mM phosphate which is parallel above 500 μM PPAPS. Therefore there are additional phosphate binding sites which can not be occupied by PPAPS. Nevertheless, at 30 mM phosphate PPAPS is still able to displace chloride although less so than in the absence of phosphate. In the presence of 75 mM phosphate an unexpected increase of chloride binding can be observed up to 50 μM PPAPS which we can not explain at present. Apart from this effect there is still a small decrease of chloride line width with increasing PPAPS concentrations thereafter. The data for the semi-reciprocal plots of Fig. 6 have been evaluated in the same way as in Fig. 4. For clarity we have only included the data for zero and 75 mM phosphate, respectively. The initial steep slope of the titration curve in the absence of phosphate reflecting the binding of PPAPS to its high-affinity binding site gradually disappears with increasing phosphate concentrations whereas the slope at high PPAPS concentrations is not affected to a great extent. It follows that the high-affinity PPAPS binding site is also a

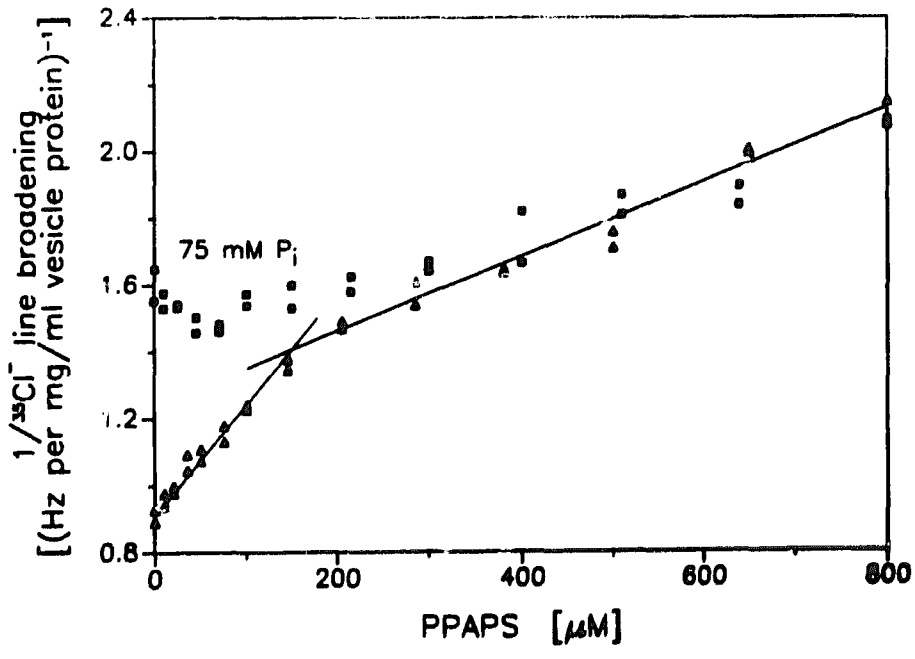

Fig. 6. Semi-reciprocal presentation of the PPAPS titrations in the presence and absence of 75 mM phosphate. ■, Presence of 75 mM phosphate; ▲, absence of phosphate. Both were carried out in the presence of 10 mM total Mg^{2+}. Data were processed as in Fig. 4.

high-affinity phosphate binding site though with a much higher apparent K_1.

Titration of nucleotide binding sites

Anion binding to the SR membrane is likely to involve the Ca^{2+}-ATPase that makes up between 50 and 90% of the total SR-protein [32,33] depending on which part of the sarcoplasmic reticulum membrane the vesicles are derived from [34]. Therefore we attempted to investigate the binding of ATP as an anionic substrate. A prerequisite for this experiment is the stability of ATP during the titration. We used ^{31}P-NMR measurements to detect formation of ADP and inorganic phosphate [35]. The half-life of Ca^{2+}-independent ATP-hydrolysis to ADP and phosphate was determined as 15 minutes (not shown). Considering that titrations of SR vesicles with ATP (measuring ^{35}Cl-NMR) last 4 h we had to replace ATP by a stable non-hydrolyzable analogue, e.g. AMP-PNP.

Fig. 7 shows AMP-PNP titrations in the presence and absence of Mg^{2+}. Because of the complexation of Mg^{2+} by AMP-PNP the free Mg^{2+} concentration was kept constant (10 mM). The K_d value of MgAMP-PNP was determined as 24.5 ± 2.2 μM (not shown). We find a smaller amount of chloride displaced in the presence of Mg^{2+}. Due to the Mg^{2+}-effect the initial value of line broadening is higher than without Mg^{2+}. The semi-logarithmic plot (inset of Fig. 7) shows that chloride displacement in the absence of Mg^{2+} stretches over a concentration range of three orders of magnitude starting at 10 μM AMP-PNP, whereas chloride displacement in the presence of Mg^{2+} happens in a narrower concentration range reaching from 0.1 mM to 5 mM AMP-PNP. The respective K_1 values are 24 ± 5 and 600 ± 100 μM in the absence, and 390 ± 50 μM in the presence of Mg^{2+}. This has been confirmed by Eadie-Hofstee analysis.

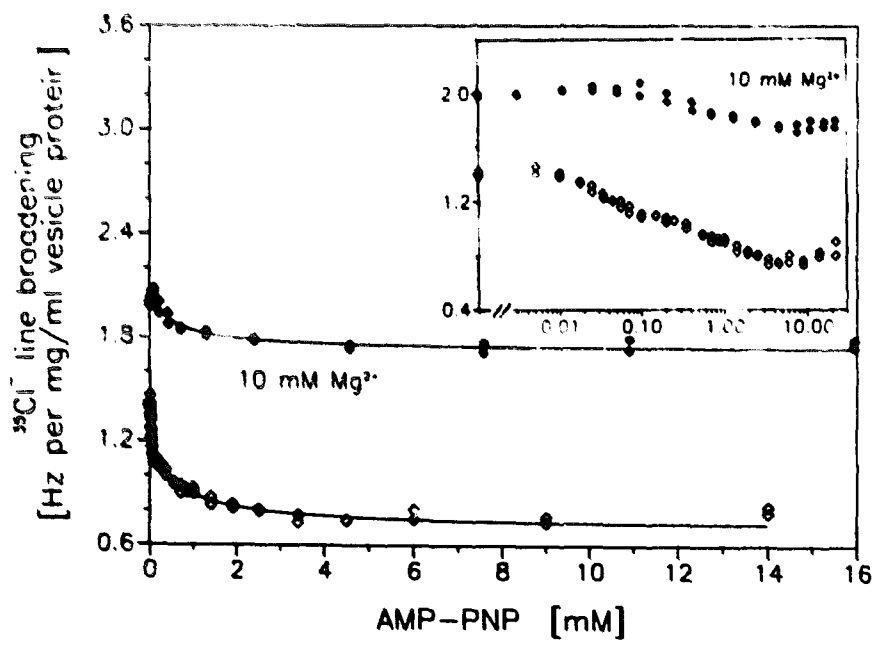

Fig. 7. Dependence of ^{35}Cl line broadening on the AMP-PNP concentration. ◆, Presence of 10 mM free Mg^{2+}; ◇, absence of Mg^{2+}. The inset shows a semi-logarithmic presentation of the data.

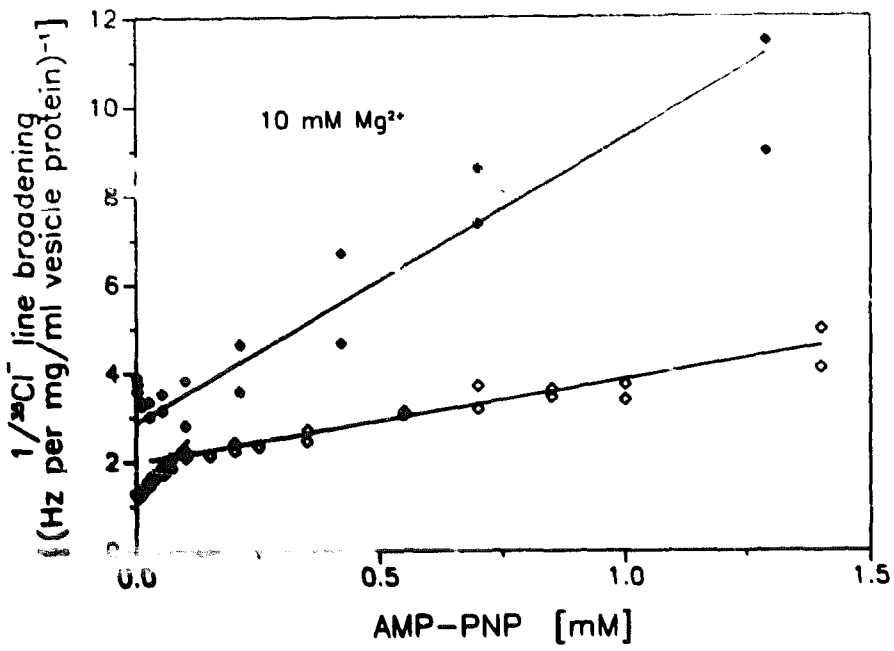

Fig. 8. Semi-reciprocal presentation of Fig. 7. ◆, Presence of 10 mM free Mg^{2+}; ◇, absence of Mg^{2+}. Data were processed as in Fig. 4.

The lower curve of the semi-reciprocal plot (Fig. 8) measured in the absence of Mg^{2+} shows a steep slope up to 100 μM AMP-PNP probably corresponding to the displacement of chloride from a high-affinity nucleotide binding site. It is followed by a less steeper slope probably reflecting a binding site of lower affinity. Therefore we think that in the absence of Mg^{2+} chloride is displaced by AMP-PNP from two different sets of binding sites, while in the presence of Mg^{2+} from one site only.

This is contrary to what has been found for the Mg^{2+} dependence of ATP binding [36] which is enhanced in the presence of Mg^{2+}. In the absence of Mg^{2+} the high-affinity K_d value of ATP and the measured K_1 value of AMP-PNP are roughly the same. Unexpectedly we find only one binding site for AMP-PNP in the presence of Mg^{2+} with moderate affinity. This is supported by the data of Pick [37] who found the apparent affinity of AMP-PNP binding decreased in the presence of Mg^{2+} (5 mM). This effect could be due to Mg^{2+}-induced changes of either the nucleotide binding site or of the AMP-PNP conformation which could result in weaker binding.

Titration of AMP-PNP in the presence of PPAPS

To find out whether PPAPS and AMP-PNP occupy the same binding sites AMP-PNP titrations were carried out in the presence of different PPAPS concentrations as presented in Fig. 9. They were performed in the absence of Mg^{2+} because AMP-PNP complexes Mg^{2+} whereas PPAPS does not. The high-affinity AMP-PNP binding site can be occupied by 50 μM PPAPS so that no chloride displacement happens up to 100 μM AMP-PNP. The curves in the presence of up to 100 μM PPAPS coincide when AMP-PNP is titrated to higher concentrations where chloride is displaced from a second binding site of lower affinity for AMP-

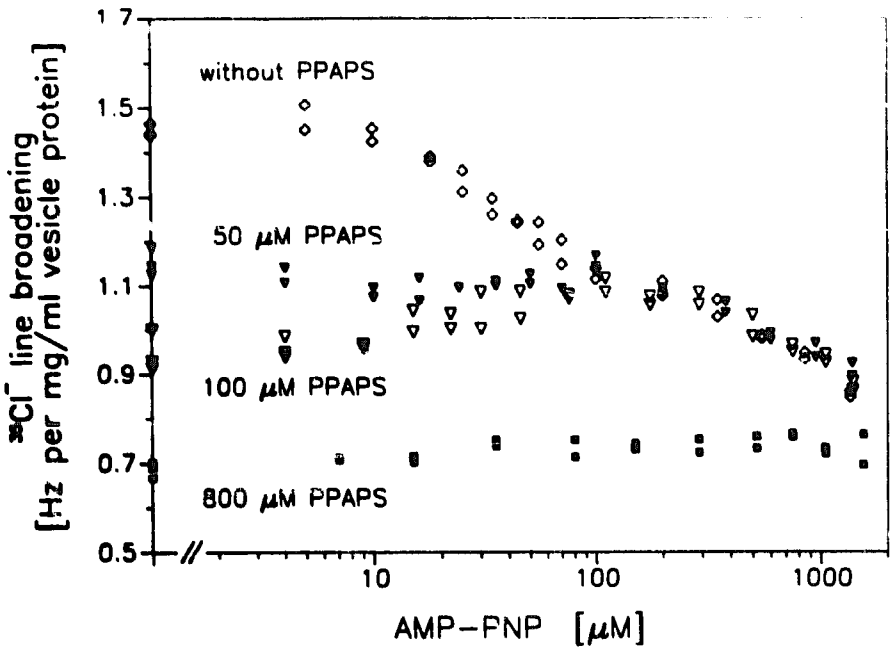

Fig. 9. Titration of AMP-PNP in the presence of different PPAPS concentrations. All titrations were performed in the absence of Mg^{2+}. Presence of ■ 800 μM; ▽, 100 μM; ▼, 50 μM. Absence of PPAPS: ◇.

PNP. Addition of 800 μM PPAPS seems to displace all chloride from AMP-PNP-sensitive binding sites. According to this data high-affinity binding of PPAPS and AMP-PNP happens at the same binding site. The same is true for the low-affinity binding sites.

Conclusions

The line broadening of the ^{35}Cl-NMR signal upon binding of chloride to a macromolecule was used as a quantitative measure for the investigation and characterization of various ligands to common binding sites on the SR membrane. In a previous publication we could already distinguish between two different sets of binding sites for chloride and several other anions [23]. The most prominent result of the present work is the extension of our previous model by defining an additional anion binding site taking advantage of the effect of Mg^{2+}. Three sets of chloride binding sites were characterized according to the relative binding strength of phosphate, PPAPS, and AMP-PNP with respect to the Mg^{2+} sensitivity. The results of our NMR experiments are summarized in Table I.

TABLE I

Anion binding sites on the SR membrane

++, high-affinity binding; +, low-affinity binding; −, no binding.

Ligand	Binding site		
	I	II	III
Phosphate	+	− [a]	+
PPAPS	++	+	−
AMP-PNP	++	+	−
Enhancement of Cl^- binding by Mg^{2+}	no	no	yes

[a] Very weak binding of phosphate (if at all).

For the transport inhibitor PPAPS we found two binding sites of different affinity (Fig. 4) where chloride binding is not sensitive to Mg^{2+}. These sites are designated site I and II, respectively. The former represents the high-; the latter the low-affinity PPAPS binding site both not being sensitive to Mg^{2+} which is confirmed in Fig. 2 where the Mg^{2+} titration curves in the presence and absence of PPAPS are the same apart from a constant shift of line broadening throughout the titration.

A significant enhancement by Mg^{2+} of chloride binding at low phosphate concentrations is shown in Fig. 1. The maximal amount of chloride displaced by increasing concentrations of phosphate is larger in the presence of Mg^{2+}. We conclude that Mg^{2+} enhances chloride binding to a third anion binding site (site III in Table 1). It is accessible to phosphate but not to PPAPS because titrations of SR with PPAPS (Fig. 3) show the same curves apart from a constant shift due to activation of site III. This is also confirmed by the data in Fig. 2.

Nevertheless, there is a binding site where phosphate and PPAPS compete (Fig. 5). Detailed analysis using a semi-reciprocal plot (Fig. 6) reveals that phosphate binds to the high-affinity PPAPS binding site (site I). This differentiation of at least two phosphate binding sites is only possible on grounds of their Mg^{2+} sensitivity.

For AMP-PNP we also find two binding sites. Apparently this is reduced to weaker binding ($K_1 = 390$ μM) to one site only in the presence of Mg^{2+} (Figs. 7 and 8). Therefore AMP-PNP binding is not comparable to that of ATP. This contrast will be studied further in a subsequent communication using other ATP analogues.

Fig. 9 shows that the high-affinity PPAPS binding site can also be assigned to high-affinity AMP-PNP binding. As a consequence this site is also accessible to phosphate (see Figs. 5 and 6). Moreover, the low-affinity AMP-PNP binding site coincides with the low affinity binding site of PPAPS. This competition study verifies the assumption made in a previous publication [22] that PPAPS affects nucleotide binding sites.

Acknowledgements

This work was supported by a grant from the Deutsche Forschungsgemeinschaft. We wish to thank Dr. H. Rüterjans for providing ample measuring time on the NMR machine.

References

1 Yamamoto, T. and Tonomura, Y. (1967) J. Biochem. 62, 558–575.
2 Makinose, M. (1969) Eur. J. Biochem. 10, 74–82.
3 Vianna, A.L. (1975) Biochim. Biophys. Acta 410, 389–406.

4 Shigekawa, M., Dougherty, J.P. and Katz, A. (1978) J. Biol. Chem. 253, 1442–1450.
5 Shigekawa, M. and Dougherty, J.P. (1978) J. Biol. Chem. 253, 1451–1457.
6 Shigekawa, M. and Dougherty, J.P. (1978) J. Biol. Chem. 253, 1458–1464.
7 Souza, D.O. and De Meis, L. (1976) J. Biol. Chem. 251, 6355–6359.
8 Punzengruber, C., Prager, R., Kolassa, N., Winkler, F. and Suko, J. (1978) Eur. J. Biochem. 92, 349–359.
9 Kolassa, N., Punzengruber, C., Suko, J., and Makinose, M. (1979) FEBS Lett. 108, 495–500.
10 Prager, R., Punzengruber, C., Kolassa, N., Winkler, F. and Suko, J. (1979) Eur. J. Biochem. 97, 239–250.
11 Nagasaki, K. and Kasai, M. (1981) J. Biochem. 90, 749–755.
12 Stephenson, E.W. (1981) Fed. Proc. 40, 2662–2666.
13 Rousseau, E. (1989) J. Membr. Biol. 110, 39–47.
14 Rousseau, E., Roberson, M. and Meissner, G. (1988) Eur. Biophys. J. 16, 143–151.
15 Beil, F., Von Chak, D., Hasselbach, W. and Weber, H. (1977) Z. Naturforsch. 32c, 281–287.
16 Chu, A., Tate, C.A., Bick, R.J., Van Winkle, W.B. and Entman, M.L. (1983) J. Biol. Chem. 258, 1656–1664.
17 Chu, A., Bick, R.J., Tate, C.A., Van Winkle, W.B. and Entman, M.L. (1983) J. Biol. Chem. 258, 10543–10550.
18 Eich, R., Illig, G., Heider, P. and Bäumert, H.G. (1992) Eur. J. Biochem., in press.
19 Falke, J.J., Pace, R.J., and Chan, S.I. (1984) J. Biol. Chem. 259, 6472–6480.
20 Lundberg, P., Vogel, H., Drakenberg, T., Forsen, S. Amiconi, G., Forlani, L. and Chiancone, E. (1989) Biochim. Biophys. Acta 999, 12–18.
21 Wydrzynski, T., Ångström, J., Baumgart, F., Renger, G. and Vänngård, T. (1990) Biochim. Biophys. Acta 1018, 55–60.
22 Vetter, I.R., Hanssum, H. and Bäumert, H.G. (1988) Biochim. Biophys. Acta 945, 11–16.
23 Vetter, I.R., Hanssum, H. and Bäumert, H.G. (1991) Biochim. Biophys. Acta 1067, 9–16.
24 Hasselbach, W. and Makinose, M. (1963) Biochem. Z. 339, 94–111.
25 De Meis, L. and Hasselbach, W. (1971) J. Biol. Chem. 246, 4759–4763.
26 Laemmli, U.K. (1970) Nature 227, 680–685.
27 Gornall, A.G., Bardawill, J. and David, M.M. (1949) J. Biol. Chem. 177, 751–766.
28 Fiske, C. and SubbaRow, Y.P. (1925) J. Biol. Chem. 66, 375–400.
29 Martonosi, A. and Feretos, R. (1964) J. Biol. Chem. 239, 648–658.
30 Forsén, S. and Lindman, B. (1981) in Ion Binding in Biological Systems as Studied by NMR Spectroscopy, Methods Biochem. Anal. 27, 289–487.
31 De Meis, L. (1989) Biochim. Biophys. Acta 973, 333–349.
32 Hasselbach, W. (1978) Biochim. Biophys. Acta 515, 23–53.
33 Berman, M.C. (1982) Biochim. Biophys. Acta 694, 95–121.
34 Meissner, G. (1975) Biochim. Biophys. Acta 389, 51–68.
35 Cohn, M. and Rao, B.D.N. (1979) Bull. Magnet. Reson. 1, 38–60.
36 Moller, J.V., Lind, K.E. and Andersen, J.P. (1980) J. Biol. Chem. 255, 1912–1920.
37 Pick, U. (1981) Eur. J. Biochem. 121, 187–195.